Hydrogeochemical and Microbiological Studies for Enhanced Groundwater Bioremediation

Madeline E. Schreiber and Jean M. Bahr, Dept. of Geology and Geophysics, UW-Madison

Michele D. Zwolinski, Environmental Toxicology Center, UW-Madison

Yan Shi and William J. Hickey, Dept. of Soil Science, UW-Madison

Acknowledgments

I. Introduction

Contamination of shallow aquifers by dissolved aromatic hydrocarbons resulting from leaking underground storage tanks is a widespread problem. Of particular concern are the BTEX (benzene, toluene, ethylbenzene, and xylenes) compounds because they are both toxic and highly mobile in groundwater. Bioremediation is often considered for treatment of hydrocarbon-contaminated groundwater. Because electron acceptor demands typically created in aquifers following fuel contamination greatly exceed dissolved oxygen supplies (Chapelle et al., 1995), contaminated aquifers naturally tend to become anaerobic. Biodegradation processes operative under anaerobic conditions are thus important for supporting intrinsic bioremediation. Anaerobic processes have also been considered for potential use in enhanced bioremediation to avert difficulties associated with introducing, dispersing, and maintaining oxygen at levels adequate to sustain aerobic biodegradation (National Research Council, 1994). For these applications, electron acceptor supplementation with nitrate has attracted particular attention because of its high water solubility and general lack of noxious by-products (Hutchins et al., 1991; Batterman, 1986; Reinhard et al., 1997).

Elucidation of the microbiological and hydrogeochemical influences on anaerobic biodegradation of hydrocarbons in aquifers is needed to gain an improved understanding of both intrinsic and enhanced bioremediation processes (National Research Council, 1994). The main objectives of this study were to examine processes involved in anaerobic biodegradation through field and laboratory experiments and to incorporate results into numerical modeling to more accurately predict biodegradation. Specific tasks associated with these were to 1) evaluate the extent of biodegradation that occurs naturally in the plume (intrinsic bioremediation) through field monitoring; 2) conduct tracer tests to evaluate if addition of electron acceptors, specifically nitrate and sulfate, enhances biodegradation and, if so, to quantify rates; 3) construct microcosm experiments to test specific processes and to examine degradation under sequential electron-accepting processes; and 4) use computer models to simulate the current and possible future configurations of the BTEX plume.

II. Site characterization: Implications for intrinsic bioremediation

Introduction

The distribution of the dominant electron-accepting processes in groundwater contaminated with benzene, toluene, ethylbenzene, and xylenes (BTEX) has a significant influence on biodegradation rates and the susceptibility of the different BTEX compounds to biodegradation (*e.g.* Borden et al., 1995). Studies of BTEX biodegradation under aerobic (Barker et al., 1987), nitrate-reducing (Hutchins, 1991; Barbaro et al., 1992; Major et al., 1988), iron-reducing (Anderson et al., 1998; Lovley et al., 1994; 1996), sulfate-reducing (Beller et al., 1992) and methanogenic (Wilson et al., 1990) conditions show that the susceptibility to degradation of individual BTEX compounds and their associated degradation rates are specific to the electron acceptor.

Most previous spatial analyses of redox zones in contaminated aquifers have been based on the assumption that the development of anaerobic conditions can be fully attributed to the presence of the introduced contaminants. For many sites, this assumption is valid because contaminant plumes are often contained within shallow aquifers that were once aerobic due to low organic matter and continuous infiltration of oxygenated recharge. Few studies have directly

3

compared the redox patterns between pristine and contaminated groundwater at the same field site to examine if an electron acceptor demand exists in systems in the absence of contaminants.

In this study, we evaluated spatial variations of redox patterns in both pristine and BTEX-contaminated portions of a shallow wetland aquifer at Fort McCoy, WI. Results of this comparison show that both pristine and contaminated groundwater have several distinct geochemical zones that are controlled primarily by microbially-mediated reactions. Although BTEX and other organic compounds in the contaminant plume exert the highest demand for electron acceptors, the oxidation of natural organic matter in the wetland also contributes to reduction of oxygen, nitrate, and mineral-bound Fe(III). Consumption of these electron acceptors in the pristine portion of the aquifer suggests that organic matter is an additional electron donor, which is likely competing for electron acceptors in the plume.

Field site. The field site for this research is located at Fort McCoy, in Monroe County of west-central Wisconsin (**Figure 1**). The field site is contaminated with BTEX from two 12,000-gallon leaking underground storage tanks (USTs) that were installed in 1943 and removed in 1989. Residual non-aqueous phase liquid (NAPL) in the saturated zone provides a continual source of BTEX to groundwater. The current plume is approximately 110 m long and 30 m wide at its maximum, with dissolved BTEX concentrations generally less than 20 mg/l (Figure 1). The upgradient portion of the plume is located in a grass-covered upland while the downgradient portion of the plume migrates through a forested wetland and ultimately discharges to Tarr Creek, a shallow stream. BTEX has not been detected in flowing creek water, presumably due to dilution and volatilization.

The shallow aquifer at the field site contains deposits of moderately- to well-sorted sand stratified with discontinuous silt lenses derived from the weathering of sandstones of the Lower Cambrian Elk Mound Group and reworked by local streams. A coarse sand layer occurs at approximately the same depth as the water table. In the wetland area, a 0.5- to 1-m thick layer of dark, organic soil is present near the surface and generally increases in thickness towards the creek. Discontinuous lenses of organic-rich silt are also present underlying the surficial organic soil in the wetland. Hydraulic conductivities of the sand deposits, based on slug test and tracer test results, average 8 m/d. The horizontal hydraulic gradient is approximately 0.02 in the upgradient area and approximately 0.01 in the wetland. The direction and magnitude of the horizontal gradient does not significantly vary between dry and wet periods. Vertical gradients, measured in multilevels with a manometer connected to a vacuum pump, varied across the site. Although gradients cannot be quantified precisely using this method, relative differences were used to estimate if gradient directions were positive (downward flow) or negative (upward flow). Vertical gradients were positive in the source area, while negative gradients were detected next to the creek. Between these areas, vertical gradients were slight and spatially variable.

Methods

Instrumentation. The field site is instrumented with eight monitoring wells, eighteen miniature multilevel samplers of the type described by Stites and Chambers (1991), and four larger bundle-type multilevel samplers. Seven of the eight monitoring were previously installed (RUST Inc., 1994) and have been sampled for BTEX since 1990 and for BTEX and selected redox parameters (nitrate, Fe(II), and sulfate) since 1995. The multilevel samplers are located along two transects parallel to approximate groundwater flow directions: one through a pristine portion of the aquifer (A-A'; **Figure 1**) and one through the area of the hydrocarbon plume (B-B';

Figure 1). The multilevels were sampled for various parameters during seven sampling events.

Sampling and Field Analysis. Prior to sampling, each level of the multilevel samplers was purged with a peristaltic pump at a rate of approximately 100 ml/min for 4-6 min to allow for temperature and specific conductance to stabilize. Oxidation-reduction potential (ORP), pH, temperature, and specific conductance were then measured using electrodes. In contaminated samplers, BTEX samples were collected in 40 ml vials. Hydrochloric acid was added to the vials before the samples were collected. Methane samples were collected in 40 ml vials which were filled with approximately 30 ml of groundwater. Multilevels were then sampled for field analysis of dissolved oxygen (DO), nitrate, Fe(II), and alkalinity using colorimetric methods (CHEMets, Chemetrics Inc.). Sulfate was analyzed in the field by precipitation with barium chloride and analysis on a portable colorimeter (Hach model DR100, Hach Inc.) or by ion chromatography. Samples for sulfate, dissolved inorganic carbon and dissolved organic carbon (DIC/DOC) analyses were filtered with a 0.45 μm filter.

Laboratory analysis. BTEX concentrations were determined either by headspace analysis (EPA method SW846, 8000A) on a portable gas chromatograph (GC) (HNu model 311D) instrumented with a photoionization detector or by purge-and-trap concentration (EPA method SW846, 5030) followed by analysis (EPA Method SW846, 5015) on a GC (Varian 3600) instrumented with a flame ionization detector. For headspace analysis, the sample vial was first placed upside down in a water bath at 40°C for 10 minutes, vigorously agitated for one minute, and returned to the water bath for an additional 2 minutes. Headspace (100 μl) was then removed using gas tight glass syringes and injected directly into the GC. The detection limit was approximately 0.01 mg/l. For the purge-and-trap method, 1 ml of sample was purged and concentrated prior to injection into the GC. The detection limit for this method was approximately 0.005 mg/l. For both methods, individual BTEX compounds were quantified by comparison of detector response and retention times with known standards. Differences between duplicate samples were typically less than 10%. Methane headspace samples were analyzed on a GC (Varian 3300) instrumented with a thermal conductivity detector. Samples were calibrated to a standard gas mixture of N_2 (23%), CH_4 (50%), H_2 (2%), and CO_2 (25%). Initial methane liquid-phase concentrations were calculated from final gas-phase concentrations using Henry's Law and mass balance relationships. Sulfate samples were analyzed by ion chromatography by the University of Wisconsin Soil and Plant Analysis Laboratory (UWSPL). DIC/DOC was determined by acidification (DIC) and persulfate digestion (DOC) with an OI Model 700 carbon analyzer.

Results

Geochemical Patterns in the Pristine Region. Average concentrations of the redox parameters DO, nitrate, Fe(II), and sulfate vary spatially along the pristine transect, with significant vertical stratification over intervals of a meter or less. For this discussion, we consider three zones defined approximately by depth below the water table in the upland area: a shallow zone (0 to 2 m below the water table), an intermediate zone (2 to 7 m), and a deep zone (below 7 m).

Along the pristine transect from MLA3 to ML3, four geochemical signatures can be identified: shallow upland, shallow wetland, intermediate, and deep (**Table 1**). An example of the general pattern of geochemical profiles is shown for the April 1998 sampling (**Figure 2**). In the upland area, shallow groundwater is aerobic (4 to 5 mg/l of DO), and contains nitrate concentrations (as NO_3^-) less than 6 mg/l. Fe(II) concentrations are less than 1 mg/l and sulfate

concentrations average 12 mg/l. DO and nitrate decrease along the flowpath, resulting in lower concentrations in shallow wetland groundwater. The utilization of these electron acceptors can be attributed to the presence of dissolved and sediment organic matter in the shallow zone. Concentrations of dissolved organic carbon (DOC) in shallow pristine groundwater reach almost 8 mg/l in the wetland. DOC concentrations do not decrease systematically along the flowpath, presumably because shallow groundwater is constantly replenished with organic matter from the wetland peat. Along the flowpath, dissolved Fe(II) concentrations remain low and sulfate does not appear to be significantly depleted, indicating that the supply and replenishment of DO and nitrate are sufficient to prevent the onset of iron and sulfate reduction.

In the intermediate zone, groundwater has lower DO (less than 3 mg/l) and higher nitrate concentrations. DOC concentrations in the intermediate zone reach up to 14 mg/l and systematically decrease along the flowpath. Profiles of Fe(II) and sulfate concentrations in this zone are similar to the shallow zone. Deep groundwater is anaerobic (less than 1 mg/l of DO) throughout the flowpath and contains low to undetectable nitrate and high Fe(II), up to 18 mg/l. Sulfate concentrations range from 17 to 38 mg/l at depth. DOC concentrations are less than 2 mg/l. The lack of DO and nitrate in addition to the high Fe(II) concentrations suggests the occurrence of organic matter oxidation coupled to the consumption of DO, nitrate, and mineral-bound Fe(III). Because the deep portion of the aquifer is not recharged within the area of the field site, DO and nitrate are not replenished along the flowpath. Once DO and nitrate are depleted, the next preferred and available electron acceptor is mineral-bound Fe(III). Sulfate reduction does not appear to occur in pristine groundwater, likely because concentrations of DOC and sediment organic matter load are not high enough to exhaust the Fe(III) reservoir in the pristine portion of the aquifer.

Spatial Patterns of BTEX. The source of the dissolved BTEX concentrations in groundwater at the site is a 1- to 1.5-m interval in saturated zone contained within a 100 m^2 area, located 10 m downgradient of the former tank locations (**Figure 1**). In this area, concentrations of total BTEX in sediment exceed 500 mg/kg. Dissolved BTEX data collected since 1990 from the sampling of 1.5- and 3-m screened monitoring wells (RUST, Inc. 1994; Brownell, 1997) indicate that BTEX concentrations appear to be systematically decreasing in some areas of the plume (MW2 and MW3), fluctuating over several orders of magnitude in other portions of the plume (MW5), and remaining relatively steady in yet other areas (MW4). The fluctuating concentrations in MW5 are directly correlated to fluctuations in water level. Because this well is located in a low-lying area and the sediments have a high silt content, the cause of the fluctuating BTEX concentrations is likely due to residual saturation in sediment near the water table.

Data from multilevel samplers collected between 1995 and 1997 as part of this study (**Table 2**) indicate that the dissolved BTEX plume is 2 to 3 m thick (**Figure 3**). The highest BTEX concentrations occur approximately 0.5 to 1 m below the water table along the length of the flowpath, likely due to infiltration of focused recharge in the ditch next to the road, near MLA2. The plume does not sink further in the wetland, where recharge is limited by vegetation and flow is essentially horizontal. Near and beneath the stream, strong upward gradients persist and cause the plume to discharge into the stream. Elevated BTEX concentrations extend to the shallow zone of the multilevel adjacent to the creek (ML4) but only trace concentrations (<0.001 mg/l benzene, below the quantitation limit) have been measured in the shallow intervals of the streambed multilevel (MLS-1). One sample collected at the creek bank had detectable benzene

(0.002 mg/l), suggesting that the plume is also discharging at the seepage face. BTEX has not been detected in flowing creek water, presumably due to dilution and volatilization. No underflow is thought to occur because samples collected from a multilevel sampler installed on the other side of the creek (ML79) showed no detectable BTEX.

Geochemical Patterns in the Contaminated Region. Groundwater in the intermediate and deep zones along the contaminated transect displays geochemical trends similar to intermediate and deep zones of pristine groundwater; however, the presence of BTEX in the shallow zone causes significant changes in groundwater chemistry (**Table 3**) due to microbially-mediated biodegradation reactions. An example of the general pattern of geochemical profiles is shown for the April 1998 sampling event (**Figure 4**). In the shallow zone, DO and nitrate concentrations are less than 0.5 mg/l compared to the concentrations up to 5 and 6 mg/l, respectively, in the shallow zone of the pristine transect. Fe(II) concentrations in the BTEX plume reach 40 mg/l due to microbial reduction of mineral-bound Fe(III). Sulfate is depleted, but only in the zones of highest BTEX. Low concentrations (< 5 mg/l) of methane were detected only in these high BTEX zones in which sulfate depletion was measured. Groundwater samples were analyzed for H_2S; in general, only low concentrations (less than 1 mg/l) were detected, even in zones of highest BTEX. Because of the high Fe(II) concentrations in these zones, it is likely that H_2S and HS^-, which are the by-products of sulfate reduction, are removed via precipitation to form Fe(II)-sulfides.

In the less-contaminated intermediate zone where BTEX is less than 0.05 mg/l, DO concentrations are depressed, as are nitrate concentrations. Some iron reduction occurs, as evidenced by Fe(II) concentrations up to 20 mg/l. Sulfate concentrations are similar to those in intermediate pristine groundwater and do not appear to be depleted. In the deep zone, which contains very low concentrations of BTEX (less than 0.03 mg/l), the electron acceptor profiles are generally similar to pristine profiles, except that Fe(II) concentrations are higher, up to 30 mg/l, as compared to 18 mg/l in the pristine deep zone.

Discussion

The spatial variations in electron acceptors described above have implications for calculation of assimilative capacity (AC), which is used to assess the potential for intrinsic biodegradation of a plume (Wiedemeier et al., 1995). AC is defined as the amount of the contaminant that can be potentially degraded with known amounts of electron acceptors. The general procedure for calculating AC is first to estimate the amount of electron acceptors available for biodegradation by calculating the difference between background (pristine) and plume (contaminated) electron acceptor concentrations. This difference is then multiplied by the stoichiometric ratio of the mass of BTEX biodegraded to the mass of electron acceptor utilized. The result is the amount of BTEX that potentially can be biodegraded by electron acceptors in groundwater at the site.

Analytical biodegradation screening models, such as BIOSCREEN (Newell et al., 1996), explicitly employ the AC to assess biodegradation potential. More complex numerical models, such as BIOPLUME III (Rifai et al., 1998), RT3D (Clement, 1997) and BioRedox (Carey et al., 1998) calculate AC internally based on input of electron acceptor concentrations and either a hard-wired or user-defined stoichiometric coefficient. Because AC estimates are used in both screening and numerical models to simulate biodegradation, it is important to assess the applicability of the assumptions incorporated into the calculations. Two of these, in particular, can lead to significant errors if they are not appropriate for the site of interest. The first is that

electron acceptors do not vary spatially. The second, manifested in use of the stoichiometric mass ratio, is that electron acceptor depletion in the plume can be fully attributed to BTEX biodegradation.

The Fort McCoy study provides an example of a site where there is significant spatial variability in background electron acceptor concentrations and where natural organic matter can cause significant depletion of electron acceptors. Thus, the location at which electron acceptor concentrations are measured is crucial to the AC estimates.

Spatial Variation in Electron Acceptors. Results of multilevel sampling indicate that electron acceptor concentrations vary both laterally and vertically at this site. The vertical variability is not captured by monitoring wells that are screened over multiple groundwater zones. **Figure 5** compares electron acceptor and BTEX profiles for a monitoring well (MW8) to those of a multilevel sampler (MLA4) in the plume. Profiles from the multilevels clearly show where the steep concentration gradients occur with respect to both electron acceptors and contaminants. Because the monitoring well MW8 is screened both in and below the plume, samples collected from this well provide misleading information on concentrations of both electron acceptors and BTEX. This example shows the importance of delineating the zone of interest and then installing monitoring equipment that yields physical and chemical data representative of the zone of interest.

The zone of interest at this field site, the BTEX plume, is contained within the shallow groundwater zone. Errors in AC estimates can arise if they are based on data from monitoring wells that are screened over multiple groundwater zones or if the samples are collected from a completely different groundwater zone. To demonstrate these potential errors, eleven estimates of AC using different combinations of data sources for the electron acceptors are shown in **Table 4**. Estimate 1 uses data from monitoring wells that are screened partially or fully through the shallow groundwater zone. Estimates 2 through 6 use data from a combination of one monitoring well and the shallow groundwater zone from a multilevel sampler. Estimates 7 through 11 use multilevel data for both background and plume concentrations. Because DO and methane concentration data were not collected from monitoring wells, the contribution of aerobic degradation and methanogenesis cannot be calculated for estimates involving monitoring wells. Therefore, in order to compare estimates between monitoring and multilevel wells, the contributions from nitrate, iron, and sulfate are summed. This term is called the AC-NIS.

Results of these AC calculations (**Table 4**) show that the different combinations of data sources result in a wide range of AC-NIS estimates. The most accurate estimates (estimates 7 and 8), which utilize average electron acceptor concentrations from the shallow zone of multilevel samplers for both the background and the plume, are 4.2 mg/l (AC-NIS) and 8 mg/l (total AC). Combinations of monitoring and multilevel well data result in AC-NIS estimates that range from 1.2 to 3.9 mg/l (estimates 2 through 6). Use of multilevel data from the incorrect (intermediate) zone results in AC-NIS estimates of 6.8, 4.5, and 0.9 mg/l (estimates 9, 10, 11). Due to mixing of highly contaminated groundwater with less contaminated groundwater, samples from the monitoring well MW5 yield lower Fe(II) concentrations and higher nitrate and sulfate concentrations than concentrations in the shallow zone of the neighboring MLA2. The overall result of this mixing is an underestimation of the AC-NIS by 75% (1.0 mg/l; estimate 1).

In addition to yielding inaccurate estimates of AC, use of spatially-inappropriate data leads to erroneous interpretations of the dominant electron-accepting processes. Based on multilevel sampler data, the highest AC contributions are from biodegradation coupled to iron

8

reduction and methanogenesis (**Table 4**). Based on monitoring well data, calculations of AC-NIS suggest that sulfate reduction is the most important electron-accepting process (**Table 4**).

Electron Acceptor Utilization Efficiency. Another potential error in calculations of AC results from the assumption that the electron acceptors are utilized to degrade only the contaminants of concern, *e.g.* BTEX. The above comparison of electron-accepting processes between pristine and contaminated groundwater is important because, although BTEX exerts the highest demand for electron acceptors, natural organic matter in the wetland also contributes to depletion of DO and nitrate. One way to characterize the electron acceptor depletion in the wetland is to calculate a zero-order rate constant. Zero-order rate constants for DO and nitrate loss were calculated based on average concentrations in shallow pristine groundwater (**Table 1**) and on an advective velocity of 0.31 m/d. If MLA1 and ML3 are used as the upgradient and downgradient data sources, the k_{DO} is 0.010 mg/l/d and the k_{NO3} is 0.008 mg/l/d. In addition to electron acceptor loss resulting from natural organic matter degradation, microbial degradation of other organic compounds in the plume will contribute to electron acceptor depletion.

If the electron acceptor demand due to natural processes observed in the pristine transect is considered in these AC calculations, the results tell a different story about the contributions of the electron acceptors (**Table 5**). The greatest effect of oxidation of natural organic matter on electron acceptor depletion is observed in the shallow zone, where DO and nitrate concentrations decrease along the pristine transect. If these losses are accounted for, the AC is lowered. For example, using shallow zone electron acceptor concentrations, the AC is decreased from 8 mg/l to 7.2 mg/l, a decrease of 12% (estimates 12 and 13; **Table 5**). Further evidence of electron acceptor utilization due to non-BTEX losses was gathered during two nitrate tracer experiments conducted at the site. Results reveal that less than 10% of the nitrate loss observed during the test can be attributed to the oxidation of BTEX compounds alone (Schreiber et al., 1997; 1999). The remaining 90% of loss is presumably due to 1) loss from oxidation of non-BTEX contaminants, 2) loss from organic matter oxidation, 3) loss from oxidation of Fe(II), and 4) nitrate uptake for cell nutrition. This decreased electron acceptor efficiency has implications for remediation systems that seek to enhance biodegradation via electron acceptor addition. Due to non-BTEX losses, the amount of electron acceptor addition required to achieve the optimal biodegradation may significantly exceed that predicted by stoichiometric relationships.

Biodegradation Potential at Fort McCoy. For the plume at the field site at Fort McCoy, the AC can be estimated based on the shallow zone electron acceptor concentrations because the plume is fully contained within the shallow zone. Even if electron acceptors are utilized to degrade only BTEX, and not other organic compounds in the plume, the total BTEX that can potentially be degraded in the shallow zone is around 8 mg/l, which is significantly less than the highest BTEX concentrations at the site (20 mg/l). If the natural processes are considered in calculations, the amount of BTEX that can be degraded decreases to around 7 mg/l. Thus, results of this study suggest that even though intrinsic bioremediation is not sufficient for complete remediation of the existing plume, it contributes to decreased BTEX concentrations in some areas of the plume.

III. Tracer experiments: Assessing potential for enhanced bioremediation

Introduction

In many petroleum-contaminated environments, intrinsic biodegradation, although it can contribute to stabilizing or containing the plume, may not be sufficient to remediate groundwater to regulatory standards due to high concentrations and/or volumes of non-aqueous phase liquid (NAPL) or slow biodegradation rates under anaerobic conditions. In such environments, the addition of electron acceptors to the plume could enhance biodegradation of the contaminants and thus speed up the treatment process.

As described in Section II, assimilative capacity calculations suggest that intrinsic biodegradation, although it may contribute to plume stabilization, is not sufficient for complete remediation of the plume at the Fort McCoy field site. For this reason, we conducted three tracer experiments in a fuel-contaminated wetland aquifer to evaluate if biodegradation could be enhanced via electron acceptor addition, and to estimate transport parameters that were required for simulation of three-dimensional flow and multi-species reactive transport at the site. The tracer experiments used bromide as a conservative tracer and nitrate or sulfate as potential electron acceptors.

Methods

Injection. The tracer tests were conducted in three biogeochemically distinct zones of the contaminated portion of the aquifer: 1) a shallow, anaerobic zone with high BTEX concentrations, 2) an intermediate, microaerophillic (< 1 mg/l DO) zone with moderate BTEX concentrations, and 3) a deep, anaerobic zone with low BTEX concentrations (**Figure 6**).

The 1996 nitrate and bromide tracer (96NB) was injected into all three zones 1) to evaluate if nitrate would be utilized in any or all of the zones and 2) if nitrate loss were measured, to compare nitrate loss rates between the different zones. Contaminated groundwater was pumped from WW1 (screened over all three zones) to the surface and into an airtight flow-through cell at a rate of approximately 800 ml/min. Concentrated tracer solution (5000 mg/l of bromide and nitrate-N) was pumped into the same cell at a rate of approximately 8 ml/min. This 1:100 dilution was intended to produce outlet tracer concentrations of 50 mg/l each of bromide and nitrate-N. The tracer was injected into IW1 (screened over all three zones). No dissolved oxygen (DO) was detected at the outlet of the cell, indicating that the mixing process did not introduce DO. Over the 20 hour injection period, the volume of injected tracer was 1000 liters.

The 1997 nitrate and bromide test (97NB) was designed to specifically test if nitrate loss was coupled to BTEX loss. In this test, groundwater from the shallow, highly contaminated zone was mixed with tracer and injected into the intermediate, moderately contaminated zone. Contaminated groundwater was pumped from WW2 (screened in the shallow zone) to the surface and into an airtight flow-through cell at a rate of approximately 750 to 925 ml/min. Concentrated tracer solution (5000 mg/l of bromide and nitrate-N) was pumped into the same cell at a rate of approximately 8 ml/min, to yield a final tracer concentration of 50 mg/l of bromide and nitrate-N. The tracer was injected into IW2 (screened in the intermediate zone). To increase the width of the tracer cloud, groundwater was also pumped from WW3 (screened in the intermediate zone) to waste. No dissolved oxygen (DO) was detected at the outlet of the cell. Over the 19.5-hour injection period, a total volume of 910 liters of tracer was injected.

The 1997 sulfate and bromide tracer test (97SB) was conducted to evaluate if BTEX, particularly benzene, would degrade under enhanced sulfate-reducing conditions. In this test, groundwater from the lower portion of the shallow, highly contaminated zone was mixed with tracer and pumped back into the same zone. This test was conducted in the shallow zone instead

of the intermediate zone to avoid interference from background sulfate. Sulfate in the shallow, highly contaminated zone was below detection limits prior to injection. Because no retardation of BTEX was observed during the nitrate test, we assumed that the BTEX would not be retarded with respect to the sulfate and bromide. Contaminated groundwater was pumped from WW4 (screened in the shallow zone) to the surface and into an airtight flow-through cell at a rate of approximately 700 ml/min. Concentrated tracer solution (5000 mg/l of bromide and sulfate) was pumped into the same cell at a rate of approximately 7 ml/min, to create an outlet tracer concentration of 50 mg/l of bromide and sulfate. No dissolved oxygen (DO) was detected at the outlet of the cell. The tracer was injected into IW3 (also screened in the shallow zone). Over the 10-hour injection period, the total tracer injected was 450 liters.

Tracer monitoring. Concentrations of tracers were measured frequently during the all three injection periods (**Table 6**). Ion-specific electrodes (ISEs) were used to measure bromide and nitrate and a field colorimetric test kit (CHEMets) was used to detect low concentrations (<5 mg/l) of nitrate-N. Due to chloride interferences, the ISEs had a detection limit of approximately 5 mg/l. Sulfate was analyzed by precipitation with barium chloride and analysis on a spectrophotometer (Hach DR 3000). This method had a detection limit of approximately 10 mg/l. Samples collected during injection and were also analyzed for bromide, nitrate, and sulfate by ion chromatography (IC) (method SW846, 9056) by the University of Wisconsin Soil and Plant Analysis Laboratory (UWSPL) and for PVOC compounds (MTBE, benzene, toluene, ethylbenzene, — and p-xylene, o-xylene, 1,2,4- and 1,3,5-trimethylbenzene, and naphthalene) by gas chromatography (method SW 846, 8021) by the Badger Analytical Laboratory.

During the monitoring period, samples were collected daily during all three tracer tests. Prior to sampling, approximately 50 ml of water was purged with a peristaltic pump. Approximately 80 ml was then collected for analysis using the ISEs (bromide and nitrate), the colorimetric test kit (low-level nitrate) or the turbidimetric method (sulfate). During the last week of the sulfate test, samples were sent to Badger Analytical for analysis by ion chromatography. Every one to two hours, the ISEs were checked against standards. The standards were kept in a cooler and were taken out 5 to 10 min. before analysis to let them warm to temperatures similar to those of the samples. Samples for BTEX (benzene, toluene, ethylbenzene, m, p-xylene, and o-xylene) analysis were collected after a 50-ml purge in 40-ml vials that were pre-preserved with hydrochloric acid. The samples were collected under low-flow conditions. The samples contained no headspace and were put on ice immediately after collection. The samples were analyzed within 5 days of collection on a gas chromatograph (Varian 3600) equipped with a purge-and-trap concentrator and a photo-ionization detector (EPA Method SW846, 5015). This method had a detection limit of approximately 25 μg/l. External standards were used for calibration.

The tracer clouds were monitored using 73 multilevel samplers, the majority of which were installed during 96NB. Each piezometer contained 10 sampling points located at 0.3-m intervals, from approximately 1.1 m below ground surface (bgs) to approximately 3.8 m bgs. Because the tracer was injected over an 2.4-m vertical interval, we were able to monitor the tracer in all three groundwater zones. The tests were monitored for 100 days (96NB), 60 days (97NB), or 30 days (97SB).

During all three experiments, water levels in monitoring wells and water table wells at the site were measured to evaluate fluctuations in the magnitude and direction of the horizontal hydraulic gradient. Vertical gradients in the tracer site area were measured using a portable

manometer attached to a vacuum pump. Although gradients could not be quantified precisely using this method, relative differences in water elevations were used to estimate if vertical gradients direction were positive (downward flow) or negative (upward flow).

Results and discussion

Tracer pathways. In general, accounting for the differences in the locations of the injection and withdrawal wells, the tracer pathways were similar for all three tests (data not shown). However, results of the 96NB test indicate that the tracer pathways for different depths varied. For example, at approximately 0.3 m below the water table (1.4 m bgs), the tracer cloud veered off to the southeast, while at deeper intervals, the cloud traveled to the southwest. The differences in tracer pathways are likely caused by the relative influences of the regional and the local hydraulic gradient. The regional gradient is toward the south-southwest while the local gradient is toward Tarr Creek (**Figure 7**).

Tracer transport occurred horizontally over much of the monitored pathway. This was expected because in general, vertical gradients were negligible across the tracer site (**Figure 7**). Based on breakthrough patterns, upward vertical tracer transport was suspected in an area approximately 10 m downgradient from injection. Subsequent measurement of vertical gradients in the multilevels indicated that negative gradients persist in ML43 and ML38 (**Figure 7**), located just upgradient from a large maple tree.

Transport properties. Transport properties, including advective velocity, retardation, and biodegradation, were evaluated from breakthrough curves of the conservative (bromide) and reactive (nitrate, sulfate) tracers. Breakthrough curves are also often used to estimate dispersion characteristics. The common analytical solutions used to model dispersion are based on either slug (instantaneous) or continuous injection. Because the 10- to 20-hour injection in our tests cannot be characterized as either slug or continuous, dispersion properties were instead used as calibration parameters in numerical modeling runs (Schreiber, unpublished data). Results of calibration of the 97NB test suggest that over the 30-m scale of the tracer experiment, the longitudinal dispersion coefficient is between 0.015 and 0.15 m, and the horizontal transverse dispersion coefficient is between 0.0015 and 0.015 m. Vertical dispersion is thought be to be negligible; all vertical tracer transport was correlated to vertical gradients.

Breakthrough curves of bromide and nitrate for the 96NB test are shown for three intervals, one interval in the shallow zone (2.3 m), one in the intermediate zone (2.6 m), and one in the deep zone (2.9 m) at four locations along the tracer path (**Figure 8**). Concentrations were normalized by dividing by the injection concentrations of 75 mg/l for bromide and 55 mg/l for nitrate-N, as read by the ion-specific electrodes (**Table 6**).

Breakthrough curves of bromide, nitrate, and BTEX for the 97NB test are shown for the intermediate zone (2.6 m) (**Figure 9**) at five locations along the flowpath. Concentrations of BTEX, bromide, and nitrate were normalized to concentrations measured in ML14 on July 9, 1997. By using concentrations from samples collected in groundwater instead of the mixing cell, any BTEX losses to volatilization or other processes that could affect concentrations between the mixing cell and groundwater were not considered in degradation calculations.

Breakthrough curves of bromide, sulfate, and BTEX for the 97SB test are shown for one interval in the shallow zone (2.3 m bgs) (**Figure 10**). Concentrations of BTEX, bromide, and sulfate were normalized to concentrations measured in ML14 on August 1, 1997.

Advective velocity. Advective velocities of the tracer at different depths were estimated by dividing the distance between two wells along the tracer path by the travel time of the peak concentration of bromide. In general, advective velocities varied slightly between the different sampling depths, ranging from 0.2 to 0.4 m/d. These lateral and vertical changes in velocity may be reflective of either subtle heterogeneities in grain sizes in the sediment or slight changes in the direction of the hydraulic gradient. Vibracores collected in upgradient (VC3) and downgradient (VC4) portions of the tracer area indicate that the depositional patterns of the fluvial sediment varied spatially. Below the water table, the aquifer is composed primarily of fine to medium-grained sand, with low silt content. Some silty zones were observed at the same elevation as the water table, which may be the cause of slightly lower velocities observed at the 1.4 m bgs level. Below a depth of 2.4 m bgs, the grain size coarsened slightly, which is likely related to higher velocities observed in the 2.6 and 2.9 m intervals.

Retardation. Based on the breakthrough patterns, there is no evidence of retardation of the nitrate, sulfate, or BTEX relative to bromide (**Figures 8, 9, 10**). In this aquifer, the organic matter content widely varies, with some of the shallow organic sediments with an organic matter content greater than 0.05, and the sandy sediments containing less than 0.005 organic matter. In the intermediate zone (2.6 m bgs), the zone of the 97NB test, the organic matter content is 0.001. In the shallow interval (2.3 m bgs), the zone of the 97SB test, the average organic matter content is 0.02. So, although portions of the aquifer contain high organic matter, the organic matter content in the tracer injection intervals does not appear to be high enough for significant BTEX sorption.

Degradation.

    Nitrate. In the 96NB test, nitrate loss with respect to bromide was apparent in the shallow, highly contaminated zone along the flowpath (**Figure 8a**). In the intermediate zone, nitrate loss was less significant, and was only apparent at the end of the flowpath (**Figure 8b**). In the deep zone with low BTEX, no nitrate loss was apparent along the flowpath (**Figure 8c**). Although nitrate loss in the deep zone was insignificant, dilution and dispersion caused nitrate-N concentrations discharging to the stream from the deep zone to be significantly less than 10 mg/l as measured in a multilevel at the stream edge. These concentrations in discharging groundwater were in compliance with the nitrate discharge requirements of the Wisconsin Department of Natural Resources.

    In the 97NB test, nitrate loss with respect to bromide was observed in the shallow, intermediate, and deep zones. In the shallow zone, we first observed nitrate loss between 1 and 3.4 m from injection. Full depletion of nitrate occurred by a distance of approximately 10 m. In the intermediate zone, significant nitrate loss was not observed until between 4.6 and 7 m from injection. Nitrate was fully depleted by a distance of approximately 11 m from injection (**Figure 9**).

    In the absence of retardation, nitrate concentrations can be compared directly to the bromide concentrations to determine the extent of nitrate loss. The ratio of the normalized nitrate concentration to the normalized bromide concentration can be used to assess if nitrate utilization is occurring and to quantify the rate constants of the utilization. On a plot of the logarithm of normalized nitrate to bromide ratio versus time (on an arithmetic scale), a straight line with a negative slope corresponds to a first-order decay process. **Figure 11** was compiled

13

using normalized NO_3-N/Br ratios from successive multilevels along the flowpath in the shallow, intermediate, and deep zones during the 96NB test.

In the shallow zone, after a lag period of approximately 7 days, the estimated rate constants for nitrate loss are similar in the 96NB (0.037 d^{-1}) and the 97NB (0.030 d^{-1}) tests. In 1996, the rate constant is lower for the intermediate zone (0.016 d^{-1}); this is likely related to the lack of previous exposure of the intermediate zone to BTEX. In 1997, the apparent lag in the intermediate zone is longer (12 days) than in 1996 (7 days), but subsequent degradation occurs at a much faster rate (0.059 d^{-1} vs. 0.016 d^{-1}). The higher rates in the 1997 experiments may be a result of 1996 exposure to nitrate. Nitrate loss was not observed in the deep zone in 1996 but was apparent in 1997. Because BTEX concentrations in this zone are very low, the lack of nitrate loss in 1996 is likely related to an inability of the microbial populations to acclimate to both high concentrations of BTEX and nitrate. In 1997, however, because the microbial populations had been exposed previously, acclimation did occur, although the rates are much lower than those associated with the shallow and intermediate zones.

Errors in these estimates arise from both measurement errors and the frequency of measurement. As discussed previously, the ISE was subject to interferences and the ISE results were highly dependent on the temperature of the standards and samples. Also, because concentrations at each location were analyzed only once per day during most of the experiment, the time associated with the peak concentration may be inaccurate by ± 1 d.

Sulfate. In the 97SB test, the breakthrough curves for bromide and sulfate show no observable sulfate loss during the course of the experiment (**Figure 10**); however, BTEX loss was measured. There are three possible reasons why BTEX degradation was measured but sulfate loss was not. The first is that the sulfate utilized to degrade the contaminants is small enough to be within experimental error. Mass balance calculations based on stoichiometric relationships show that approximately 5 mg/l of sulfate is needed to account for the BTEX loss observed. Because the samples from ML85 were analyzed by ion chromatography, the analytical results are accurate to within less than ± 0.5 mg/l. However, the variations in injection concentration over the course of the experiment (± 5 mg/l) result in a slight error in normalized concentrations because normalization is based on only one value. The second is that background concentrations of sulfate may have interfered with the injected concentrations. Normalized sulfate peaks at 7.3 and 8.2 m were higher than the bromide peaks, suggesting that background sulfate concentrations could have been adding to measured sulfate concentrations. Analysis of sulfate background groundwater from the 2.1 to 2.4 m depth by the turbidimetric method showed no detectable sulfate; however, the limit of detection with this method is 10 mg/l. Thus, there could have been background sulfate concentrations less than 10 mg/l that would have masked any sulfate reduction that was occurring.

A third explanation is that another electron acceptor, such as mineral-phase Fe(III), was being utilized instead of the added sulfate. This explanation is plausible based on results of microcosm experiments (Section V), in which toluene degradation was observed in the absence of nitrate, the only added electron acceptor. Because methane was not detected in the microcosms, these results suggest that Fe(III) in the sediments was perhaps being utilized as an electron acceptor. Although results of iron extraction show that the amount of mineral-bound Fe(III) in the plume is reduced compared to pristine sediment, it is still present in the plume.
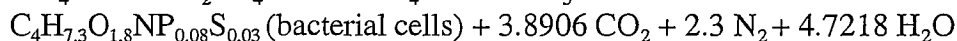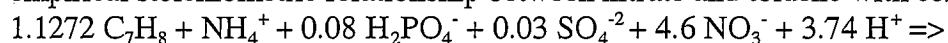
BTEX. In the 97 NB test, BTEX samples were initially collected only in the intermediate zone.

Fifteen days after injection we began to collect BTEX samples from the shallow zone. In the shallow zone, BTEX loss had already occurred by the time we began to collect samples in a multilevel 5.8 m from injection (ML33). Normalized concentrations of toluene, ethylbenzene, and m, p-xylenes were already low relative to benzene and o-xylene at ML33 and were significantly reduced at ML42, 9.8 m from injection. The BTEX loss was concomitant with a loss of nitrate, suggesting that these two reactions were coupled. Because of problems with the bromide data at late times, especially at ML42 and ML48, losses of benzene and o-xylene were difficult to assess. In the intermediate zone, BTEX loss was first observed between 4.6 and 7 m from injection (**Figure 9**). By a distance of 8.2 m, toluene, ethylbenzene, and m-, p-xylene concentrations had decreased significantly.

To evaluate if the nitrate and BTEX loss corresponded to a first-order decay process, we plotted the log of BTEX normalized to bromide vs. time on an arithmetic scale. A straight line with a negative slope suggests the degradation is proceeding under first-order decay.

In the shallow zone, BTEX loss rates cannot be calculated due to lack of BTEX data. However, losses of toluene, ethylbenzene, and m, p- xylenes were detected. In the intermediate zone (**Figure 12**), losses of toluene, ethylbenzene, and m-, p-xylenes were observed between 4.6 and 5.8 m from injection, corresponding to the time when nitrate depletion was first measured. The concentrations of these compounds were even lower at 8.2 m, at which point minor loss of o-xylene was detected. The calculated first-order rate constants were 0.019 day^{-1} for toluene, 0.012 day^{-1} for ethylbenzene, and 0.011 day^{-1} for m-, p-xylenes. A summary of the rate estimates and the lag times is presented in **Table 7**.

Mass balance calculations of the coupled reaction of nitrate reduction and TEX oxidation aid in evaluating the amount of electron acceptor needed to yield a particular loss of TEX. The empirical stoichiometric relationship between nitrate and toluene with cell production is:

$$1.1272 \ C_7H_8 + NH_4^+ + 0.08 \ H_2PO_4^- + 0.03 \ SO_4^{-2} + 4.6 \ NO_3^- + 3.74 \ H^+ =>$$
$$C_4H_{7.3}O_{1.8}NP_{0.08}S_{0.03} \text{(bacterial cells)} + 3.8906 \ CO_2 + 2.3 \ N_2 + 4.7218 \ H_2O$$

From this relationship, the stoichiometric mass ratio of electron acceptor to toluene is 2.75. Without cell production, the stoichiometric mass ratio is 4.85.

Using data collected from the intermediate zone in 97NB, the amount of nitrate and toluene, ethylbenzene, and m-,p-xylenes loss that occurred during the experiment was calculated to estimate a mass ratio of TEX degradation under nitrate-reducing conditions. The calculated mass ratio of nitrate utilized to TEX oxidized is between 91 and 156. Other field studies of BTEX degradation under enhanced nitrate-reducing conditions estimate wide ranges of this mass ratio, from 32 to 130 (Barbaro et al., 1991; Reinhard et al., 1997). These results suggest that a significantly higher amount of nitrate was needed to degrade BTEX than is predicted by stoichiometry. The possible causes of additional nitrate loss include 1) reduction coupled to oxidation of other organic compounds (besides BTEX) in the plume, 2) reduction coupled to oxidization of natural organic matter in the aquifer, or 3) reduction coupled to Fe(II) oxidation, or 4) cellular uptake. The second possibility is currently being tested in microcosm experiments.

In the 97SB test, although no sulfate loss was measured, there is evidence of BTEX degradation during the test (**Figure 10**). The BTEX breakthrough curves at ML85 (7 m from injection) show low normalized peak concentrations for m, p-xylenes, and slightly higher peaks for toluene and o-xylene. Ethylbenzene and benzene peak concentrations are highest and are similar to peak concentrations of bromide and sulfate. At 8.4 m, further loss of m, p-xylenes was measured. Ethylbenzene loss was also apparent at this location, but benzene peaks still mirror

bromide and sulfate, suggesting that benzene did not degrade, at least on the scale of this test.

Figure 12 is a plot of the logarithm of normalized BTEX to bromide ratio versus time on an arithmetic scale. Normalized benzene is similar to bromide, suggesting that it did not degrade. However, relative concentrations of toluene and all three xylenes decreased over time. First-order rate constants were estimated to be 0.045 day^{-1} for toluene, 0.048 day^{-1} for m, p-xylenes, and 0.051 day^{-1} for o-xylene (Table 7). Minor ethylbenzene loss was observed at the last monitoring location but was too small to quantify.

IV. Modeling
Introduction
Design of an enhanced bioremediation system requires spatial and temporal characterization of groundwater flowpaths, groundwater velocities, and transport parameters controlling dispersion, retardation, and biodegradation. The most efficient tool for integrating these processes is a transport model. Our initial goal for this 2-year project was to gather enough information from the field and laboratory experiments to construct a transport model that could be used in support of a design for a bioremediation system. However, more information on degradation rates and microbial preferences for degradation of individual compounds is needed before the more advanced model is constructed. This information is currently being collected from ongoing microcosm studies. Therefore, for this report, we will present results from simulations of the current configuration of the BTEX plume and redox zones performed using the Reactive Transport in Three Dimensions (RT3D) model (Clement, 1997). This modeling effort was undertaken to quantify BTEX degradation under a sequence of electron-accepting conditions similar to those observed at the field site.

Model construction and input data
A finite difference flow model was constructed for the field site using MODFLOW (McDonald and Harbaugh, 1988). The dimensions of the model are 237 m in the east-west direction and 257 m in the north-south direction. The model domain has 3 layers, 56 rows, and 49 columns, for a total of 8232 cells. The cell spacing is 5 m in most of the grid but decreases in the source area. The model layering is based on the three groundwater zones defined in Section II (shallow, intermediate, and deep). All of the three layers are contained within the unconfined alluvial aquifer. The aquifer sediments consist of medium to fine sand with silt content increasing near the creek (see Section II for more description of aquifer sediments). Hydraulic conductivity, estimated from slug tests conducted in two wells in the upland area (MW1, MW7), is approximately 12 m/d. In the wetland, a hydraulic conductivity of approximately 8 m/d was estimated from velocity measurements from the tracer tests, the hydraulic gradient, and estimates of effective porosity. An overall recharge rate of 0.0004 m/d was used; increased recharge (0.0006 m/d) was assigned to ditches on both sides of the roads. No recharge was applied to the roads. Two evapotranspiration rates were utilized, based on estimates using the water table hydrograph method (Birge, 1998). The higher rate was used for the forested wetland, while the lower rate was assigned to the grass-dominated areas. No ET was assigned to the roads. Other input data are presented in Table 8.

The northern boundary was treated as a specified head. Although the regional gradient in the shallow unconsolidated aquifer, which encompasses all three layers of this model, is oriented to the southwest towards the LaCrosse River, the local gradient is southwards Tarr

Creek (**Figure 7**). The head values along the northern boundary were based on a linear interpolation of the local gradient. The stream was represented as a specified head boundary, with stage decreasing from the eastern to western boundaries at a gradient of approximately 0.002. This gradient was based on measured stream stage near ML4 and water level measurements in ML2. The east and west boundaries were no-flow. The model was run under steady-state conditions, because the flow field was assumed not to change significantly over the simulation period of 5 years, which is the time required for the transport model to reach steady-state.

The transport code RT3D (Clement, 1997) is a generalized multi-species modification of MT3D (Zheng, 1990). RT3D has several reaction modules for simulating biodegradation of fuel hydrocarbons and chlorinated solvents. Module 3 is capable of simulating biodegradation mediated by sequential, multiple electron acceptors. The kinetics of the biodegradation are assumed to be first order with respect to the hydrocarbon concentration, while a Monod-type term is used to account for the presence or absence of the different electron acceptors. An inhibition term is used to "switch" from electron acceptor to electron acceptor. More description of this code can be found in Clement (1997).

The method-of-characteristics (MOC) was used to simulate advective transport. The northern specified head boundary was assigned as a constant concentration boundary and was used to input electron acceptors DO, NO_3^- and SO_4^{-2} into the three layers; these concentrations were averaged over a 3-year monitoring period (1995 to 1998) (**Table 8**). The initial concentrations of electron acceptors and redox by-products Fe(II) and CH_4 in all 3 layers were also input. The source of BTEX was modeled as constant concentration cells; this configuration assumes that the residual NAPL is a constant source of dissolved BTEX over the simulation period. The concentration and spatial extent of the source were estimated using results of soil sampling (DeWild 1997; this study) and groundwater sampling. The input data for RT3D and sources of the data are shown in **Table 8**.

Model calibration

The flow model was calibrated to measured heads in 9 wells, velocity magnitude, and velocity direction. Calibration was conducted by altering the hydraulic conductivity and the boundary conditions. The hydraulic conductivity of the upper portion of the model was increased from 12 m/d (measured by slug tests) to 24 m/d to account for the shallower hydraulic gradient in that area. The gradient near the stream was also altered to match the velocity magnitudes and directions to those measured in the tracer tests.

The calibrated flow field is shown in **Figure 14**. Comparison of measured heads and simulated heads is shown in **Table 9**, along with calibration statistics. For the final calibration, the absolute residual mean was within 10% of the head range. The model generally overestimated the heads in the wetland and underpredicted the head in MW2. The overestimation of heads in the southwestern portion of the wetland may be due to the no-flow boundary condition on the western edge of the model. Although the local hydraulic gradient is to the south, the regional gradient is to the southwest; there were not enough head measurements to the west of the field site to determine where the regional gradient dominated the local gradient. The spatial distribution of groundwater velocities provides a good match to the observed distribution estimated from tracer tests, approximately 0.3 m/d. In the upland area and in the wetland area away from the creek, the simulated groundwater velocity was approximately 0.4 to 0.8 m/d. Close to the creek, the velocity increased to approximately 1 m/d. In several

cells near to where the creek hits the eastern no-flow boundary, the simulated velocity was up to 2.5 m/d. We believe that this is an unrealistic artifact of the boundary. For this reason, the area of high velocity was not included in the transport model.

The transport model was calibrated to BTEX and electron acceptor concentrations averaged over a 3-year monitoring period for the multilevel wells (**Figure 15**). Instead of calibrating the model with respect to all species at each location, the calibration was accomplished by comparing concentration contours and overall shapes of the BTEX plume and of redox zones. The main parameters altered during calibration were 1) dispersivity, which controls the width of the plume, 2) degradation rates, which control BTEX and TEA concentrations, and 3) stoichiometric yield coefficients, which control TEA concentrations.

Results and discussion

Observed BTEX concentrations, which represent the average of three years of monitoring, are shown in **Figure 15**. Observed DO, NO_3^-, Fe(II), SO_4^{-2} concentrations are shown in **Figure 16**. The simulated concentration distributions of BTEX, DO, NO_3^-, Fe(II), SO_4^{-2}, and CH_4 are shown in **Figure 17**. Because methane samples were only collected from 4 samplers during one sampling event, an accurate delineation of methanogenic conditions is not available. Mass inputs, outputs, and errors are shown in **Table 10**. The mass balance errors for all species are less than 10%, which was considered to be acceptable.

In general, matches between the simulated and the observed BTEX plume and redox zones were good, especially with respect to general shapes and mass boundaries. The mass front could not be compared because the plume discharges into the creek. The simulated widths of the BTEX plume, the zones of dissolved oxygen, nitrate, and sulfate depletion, and the zones of elevated FeII and methane were narrower than the observed width. This may be a result of seasonal fluctuations in the hydraulic gradient that could not be easily simulated under steady-state conditions. The narrow simulated zones of depleted sulfate and elevated methane may also be related to inaccurate rate estimates. Because we had no site-specific estimated rate constants for degradation under sulfate-reducing or methanogenic conditions, we had to estimate these degradation rates from the literature.

There were several difficulties encountered during modeling. First, field monitoring indicates high BTEX concentrations at MW3, which are not consistent with the current placement of the source area. There are two possible explanations for this: 1) there is residual NAPL near MW3 or 2) the plume is split. Currently, we have separate lines of evidence for each of these alternatives. The evidence for the presence of residual NAPL at MW3 is that free product (170 mg/l total BTEX) was found in MW3 in 1990, about a year after the tanks were removed. Since 1990, BTEX concentrations have been slowly decreasing in MW3, suggesting that there is still some free product residing in the aquifer around the well, and that this free product is slowly dissolving over time. In the upgradient well, MW5, BTEX concentrations are directly related to the elevation of the water table. When the water table is high, BTEX concentrations are high, and when the water table is low, BTEX concentrations are low. This pattern suggests the presence of residual saturation in and around the water table, which in MW5 occurs close to the sand-peat interface. This pattern is not observed in MW3, suggesting that the high BTEX in MW3 is neither related to residual saturation in peat nor to a delayed response from high BTEX in MW5. Thus, it appears that residual product is still present in the aquifer in places other than the source area and that this is causing the high concentrations in MW3 and MW5.

Another explanation is that the BTEX plume is split due to the presence of a groundwater divide in the wetland area. We do have evidence of a groundwater divide at the tracer site, near ML5. During the tracer test, tracer at one shallow depth (1.4 m bgs) was transported to the east, while tracer at the other depths was transported either south or southwest, towards the creek meander. The reason for this may have to do with the relative influences of the local hydraulic gradient and the regional hydraulic gradient. The deeper intervals may be more strongly influenced by the southwestern regional gradient.

Because it is likely that the high BTEX concentrations at MW3 are related to complex processes that could not be accounted for in this steady-state transport model, we did not attempt to match the fluctuation concentrations in MW5 or the high concentrations in MW3.

The second difficulty encountered during modeling is related to Fe(II) concentrations. The simulated Fe(II) concentrations are much higher near the source area than are the observed Fe(II) concentrations. There are two possible explanations for this: 1) the source has spread farther downgradient than we had estimated or 2) mineral-bound Fe(III) in the source area has been depleted due to iron reduction occurring over long periods of time. The first possibility was tested by conducting additional sampling in the source area. The sampling results indicate the NAPL source resides 10 to 25 m downgradient from the former location of the tanks, which was not significantly different from our estimated location. The second possibility was tested by comparing acid-extractable sediment Fe(III) concentrations in pristine sediment to the source area sediment. Results suggest that although there is variability in extractable iron concentrations, mineral-bound Fe(III) is depleted in the source area. Thus, iron-reduction coupled to BTEX oxidation is decreasing over time in the source area.

V. Microcosm experiments

Introduction

In contaminated aquifers, anaerobic degradation of hydrocarbons is mediated by a diverse community of organisms, the nature and variety of which change in time and space. While community successions appear to be a fundamental aspect of the microbial ecology underlying anaerobic hydrocarbon biodegradation, there is relatively little information on this process. The recent development of phylogenetic probes, which may be used to detect and quantify specific taxonomically-defined groups of microorganisms without culturing, offers microbial ecologists promise for gaining new insights into microbial population dynamics. For analysis of microbial community structure in complex environments, a suite of phylogenetically-nested probes may be used to conduct "top-down" analysis of the population in hybridization assays (Amann et al., 1994). In these experiments, amounts of broad-spectrum (e.g., domain-level) probes are quantified by hybridizing to nucleic acids extracted from the environment, and the community structure is further defined in subsequent hybridization assays using probes with progressively greater specificities.

The objectives of this study were to evaluate the use of phylogenetic probes to identify alterations in aquifer microbial community structure elicited by fuel contamination. Analyses were done on fuel-contaminated and non-contaminated aquifer material taken directly from the field, and on aquifer materials used to establish anaerobic microcosms supplemented with toluene and/or nitrate. The latter experiments were done to gain information on effects of specific, isolated variables relevant to bioremediation of anaerobic aquifers, and facilitate
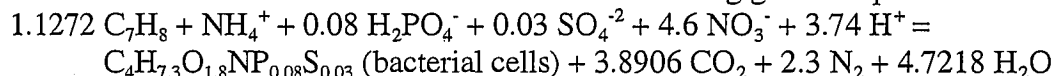
establishment of phylotype-ecotype linkages.

Materials and methods

Aquifer sampling. To obtain aquifer material samples, a Geoprobe® (Geoprobe® Systems, Salina, KS) was used to core to a depth of 1.4 m. The coring tube was retrieved, a sterile acrylic sleeve inserted, and then the device driven an additional 0.6 m into the aquifer. The acrylic sleeve was then removed, capped, sealed with duct tape, and stored on ice for transport to the laboratory. Samples were also collected from a parallel (80 m horizontal separation), pristine portion of the aquifer. Cores were used immediately for microcosm establishment and/or DNA extraction. All of these procedures were completed within 48 hours of sampling.

Microcosm experiments. Microcosms were established under an N_2 atmosphere in an anaerobic glovebox (model HE-493, Vacuums Atmosphere Co., Hawthorn, CA). These contained 50 g homogenized, sediment material from contaminated or pristine regions of the aquifer and 50 ml of base medium. The base medium was composed of 45 mg/l KH_2PO_4 and 38 mg/l NH_4Cl, adjusted to pH 7 with NaOH. Duplicate microcosms were then amended with 217 mg/l KNO_3 and/or 23 mg/l of toluene. Duplicate microcosms containing the sediment and base medium alone were used as non-amended controls. The serum bottles were sealed with Teflon-coated butyl rubber stoppers affixed with aluminum crimp caps and then incubated inverted in the dark with continuous, gentle agitation on an orbital shaker (150 RPM) at 24 °C.

During incubation, headspace and aqueous samples were taken and analyzed to track substrate consumption (toluene, NO_3^-) and product formation (NO_2^-, N_2O, CO_2). To monitor NO_2^- and NO_3^- levels, aqueous samples (0.5 ml) were periodically taken and assayed by colorimetric methods (Hanson and Phillips, 1981; Weatherburn, 1967). Additional 0.5 ml-aliquots were taken for toluene analysis. Samples for toluene were extracted into 0.5 ml of pentane. Toluene concentrations were determined using a Hewlett Packard (Palo Alto, CA) 6890A GC equipped with a Hewlett Packard 5972A mass-selective detector. Carbon dioxide and N_2O were analyzed in 1 ml headspace samples on a Hewlett Packard 5890A GC fitted with a thermal conductivity detector (TCD). The packed column-TCD method also allowed separation and quantification of CH_4, but this gas was never detected in headspace samples from the microcosms. For mass balance calculations the following growth equation was used:

$$1.1272\ C_7H_8 + NH_4^+ + 0.08\ H_2PO_4^- + 0.03\ SO_4^{-2} + 4.6\ NO_3^- + 3.74\ H^+ =$$
$$C_4H_{7.3}O_{1.8}NP_{0.08}S_{0.03}\ \text{(bacterial cells)} + 3.8906\ CO_2 + 2.3\ N_2 + 4.7218\ H_2O$$

Nucleic acid extraction and purification. Nucleic acids were extracted from the aquifer sediments and the microcosms using a modified soil extraction procedure (Tsai and Olsen, 1991). The technique involves incubating the sediment with lysozyme and then subjecting the sample to three freeze-thaw cycles (-60 to 65 °C). The nucleic acids are separated with phenol-chloroform extraction and precipitated with isopropanol. The DNA was purified from the sediment organic matter by passing through columns of Sepharose 2B (Sigma) followed by WizardTM Plus Miniprep columns (Promega). The extracted DNA was quantified by electrophoreses on 1% agarose gels stained with ethidium bromide. The sample signal was compared to a standard curve generated with lambda DNA. More details on methodology can be found in Shi et al. (1999).

Hybridization analysis. DNA extracted from the aquifer sediment and the microcosms was

applied to nylon-membranes (Amersham, Arlington Heights, IL) with a 72 well slot-blot manifold and immobilized by exposure to UV light (120 mJ). 5'-Digoxygenin labeled oligonucleotide probes were hybridized to the DNA samples. DNA extracted from both a target and a non-target reference organism was included on all blots. Hybridization signal for each probe was quantified by compassion to the hybridization signal generated by the target reference organisms. The relative abundance of domains or subgroups were determined by normalizing hybridization signals to the signal generated from hybridization to a universal probe (Fry et al., 1997; Zheng et al., 1996). Hybridization signals were analyzed with image analysis software (IPLab Gel, Sanalytics Inc., Vienna, VA).

Results and discussion

Molecular characterization of field samples. DNA yields for the contaminated sediment were higher than those for pristine sediment (**Figure 18A**). Domain probe analysis of the aquifer samples showed the DNA extracts were essentially all *Bacteria* (**Figure 18B**); *Eucarya* and *Archaea* were non-detectable (0.5 ng DNA or 0.25% of the community DNA analyzed in a typical blot). At the phylum/subclass level, the contaminated and pristine aquifer material showed similar relative abundance patterns of 43-65% $\beta+\gamma$-*Proteobacteria* (B+G) > 31-35% α-*Proteobacteria* (ALF) > 15-18% sulfate-reducing bacteria (SRB) > 5-10% high G+C Gram-positives (HGC). The suite of probes applied gave sufficiently comprehensive coverage of the community as reflected in the sums of normalized domain signals and subgroup probes (**Figure 18B**).

The dominance of *Bacteria*, and the *Proteobacteria* specifically, might have been anticipated given that organisms comprising the latter group are collectively capable of utilizing all of the TEAPs indicated by the chemical analyses of groundwater as potentially important in the contaminated and pristine zones. The only electron acceptor excluded from utilization by the *Proteobacteria* is carbon dioxide (methanogenesis). The lack of detectable *Archaea* suggested that methanogenesis was not a major process in the portion of the aquifer sampled. The most obvious difference in community structure between the pristine and contaminated regions was the greater abundance of B+G relative to ALF in the contaminated sample. This shift could be interpreted to indicate that ALF and B+G were co-dominant in the pristine aquifer but that positive- and/or negative-selective pressures imposed by fuel contamination, as well as shifting electron acceptor availability, resulted in proliferation of B+G at the expense of ALF.

Chemical and molecular analyses of microcosms: pristine sediments. Toluene supplementation stimulated microbial growth as indicated by levels of CO_2 production and DNA yields compared to the non-amended controls (**Table 11, Figure 19A**). Toluene degradation was detectable between days 10 to 12, as compared to the 5 to 15 day lag time observed in the field tracer experiments. Loss of toluene coincided with the period of enhanced CO_2 production (**Table 11**). Domain probe analysis showed that in both the toluene-amended and non-amended flasks *Bacteria* accounted for 85 to 95% of the community DNA, *Eucarya* 2 to 8%, and *Archaea* were non-detectable (**Figure 19B**). Shifts in microbial community structure were detectable at the phylum/subclass level. In the non-amended microcosm, the relative abundance was 50% B+G, 20% ALF, 15% SRB, and 2% HGC (**Figure 19B**). In the toluene-supplemented microcosms there was reversal of the ALF vs. B+G as the dominant subclass (**Figure 19B**).

Nitrate amendment also stimulated CO_2 production and enhanced DNA yields (**Table 11,**

Figure 19A). The electron donor source in this case was presumed to be native organic material. Nitrate consumption paralleled CO_2 formation and production of NO_2^- and N_2O (**Table 11**). Nitrite accumulations were greatest within the first week of incubation (4 to 12 μmoles) and subsequently steadily decreased. Production of N_2O was also detectable by the first week, and after 8 to 10 days reached a consistent level of 12 μmoles. Nitrite and N_2O were not detected in microcosms that did not receive NO_3^- supplementation. Formation of these nitrate reduction products provided evidence that populations of denitrifying organisms were stimulated. However, molecular analysis of the NO_3^--amended aquifer material showed no significant differences in community structure at the domain or subgroup level compared to the nonamended control.

Combining the amendments did not significantly increase CO_2 production or DNA yields above levels obtained with the individually-applied supplements (**Table 11, Figure 19A**). Nitrate addition supported more rapid toluene degradation compared to the microcosms spiked with toluene alone and toluene supplementation decreased levels of NO_2^- and N_2O accumulation (**Table 11**). These results suggested linkage of toluene degradation to nitrate reduction. The community structure at all the levels examined was similar to that determined for the microcosms amended with toluene alone. The suite of probes applied gave sufficiently comprehensive coverage of the microbial population as reflected in the sums of normalized hybridization signals (**Figure 19B**). For the pristine sediment, the sum of domain level signals (normalized to the universal probe) ranged from 84 to 108%, and 81 to 91% for the phylum/subclass categories.

Two lines of evidence allowed us to rule out methanogenesis as a significant TEAP. First, molar ratios of $CO_2:CH_4$ produced during chemoorganotrophic growth of methanogens might range from 1:1 to 1:3; chemolithotrophic growth results in carbon dioxide depletion and methane enrichment (Gottshalk, 1986). Given that the measured CO_2 levels were on the order of 20 to 40 μmoles (**Tables 11 and 12**), methane should have been easily detectable (i.e., >1,000-fold excess of the detection limit) even if methanogenesis accounted for only a fraction of the total CO_2 production. Second, methanogenesis could be dismissed as occurring in the nitrate-amended microcosms according to first principles of thermodynamics, namely that in an anaerobic environment dissimilatory nitrate reduction will be the dominant TEAP as long as nitrate is present at appreciable levels. The chemical analysis of the microcosms (**Tables 11 and 12**) showed this clearly throughout the course of the study.

Chemical and molecular analyses of contaminated aquifer microcosms. Toluene supplementation increased total CO_2 production to about 40 μmoles compared to about 25 μmoles in the non-amended treatments (**Table 12**). Since the theoretical CO_2 production should be about 32 μmole, this may have indicated that microbial activity was supported in part by oxidation of native organic materials. While the CO_2 analysis indicated that toluene supplementation stimulated microbial activity, there was no significant effect on DNA yield (**Figure 20A**). This result may have been attributed to the high organic matter content of the contaminated sediment interfering with DNA recovery from these materials. Toluene degradation was detectable between days 6 and 10 and coincided with the period of enhanced CO_2 production (**Table 12**). Toluene degradation was more rapid than that observed in the contaminated sediment, and may have reflected the effect of prior fuel exposure on acclimation of the microbial population. Results of domain probe analysis were similar to those of the

pristine sediment in abundance patterns, and the lack of significant treatment effects on domain abundance (**Figure 20B**). However, significant effects of toluene supplementation on community structure were detected at the lower taxonomic levels. The contaminated sediment showed a 40% decrease in B+G and 8% increase in the ALF. Most striking, however, was that the majority of the DNA (67%) was not accounted for by the phylum/subclass probes (**Figure 20B**).

In contrast to results with the pristine aquifer material, NO_3^--amendment alone did not enhance CO_2 production relative to that of the non-amended control (**Table 12**). The contaminated microcosms were similar to the pristine in patterns of NO_3^- consumption and NO_2^- /N_2O production. Nitrite and N_2O were not detected in microcosms that did not receive NO_3^- supplementation. As in the pristine microcosms, there were no significant differences in community structure between the NO_3^--supplemented and non-amended aquifer materials.

The combined amendment supported the highest level of CO_2 production through the first 16 days of incubation (**Table 12**). By day 18, cumulative CO_2 production in these flasks was still greater than either the non-amended controls or the NO_3^- amended treatments, but was the same as that in the microcosms amended with toluene alone. Similar to the pristine microcosms, there were interactions between amendments: NO_3^- addition supported more rapid toluene degradation compared to the microcosms spiked with toluene alone, and toluene supplementation decreased accumulations of NO_3^- reduction products particularly N_2O (**Table 12**). The community structure was similar to that of the contaminated microcosms amended with toluene alone (**Figure 20B**). Normalized domain signals totaled 98% while those of subgroups were only 43%.

A consistent result from phylogenetic probe analysis of the contaminated microcosms was the low balances of hybridization signals from the toluene-amended aquifer materials. This could have been explained by lack of homology between probes and the dominant phylotypes, or perhaps unknown matrix effects that interfered with hybridization. To examine the latter possibly, the contaminated microcosm extracts were spiked with genomic DNA from *Escherichia coli* as an internal standard, and then hybridized with an *E. coli*-specific probe. All *E. coli* DNA-spiked extracts hybridized to the *E. coli* probe without any significant differences in signals and there was no hybridization to the extracts not spiked with *E. coli* DNA (data not shown). Thus, the significant decrease in subgroup probe signal balances in toluene-amended microcosms was not attributable to sample matrix effects but rather indicated a major community structure shift. Specifically, the dominant phylotype(s) established following exposure to toluene constituted a minor fraction of the community in the absence of this chemical.

Identifying the phylotypes established in the toluene-amended contaminated sediment could provide insights into a segment of the microbial community important for fuel degradation. Since domain-level phylotype abundance was not affected by toluene exposure and good signal balances were obtained with the domain probes, it is reasonable to infer that these organisms were *Bacteria*. Beyond this point we can only hypothesize as to the organisms' taxonomic affiliation(s), but we believe the δ-*Proteobacteria* are likely candidates. This is because organisms within this subclass are mainly anaerobes capable of using a variety of TEAPs, and many of these might not be detected by the SRB probe. An example is Geobacter, which can grow anaerobically with monoaromatic compounds as sole carbon and energy sources, possesses a membrane-bound nitrate reductase, and is widely distributed in sedimentary

environments like aquifers (Coates et al., 1996; Lovley and Lonergan, 1990; Lovley et al., 1993; Naik et al. 1993).

Comparison of field sample analysis and microcosm experiments. At the domain level, the microbial community structure showed no significant differences regardless of the aquifer material type or microcosm amendment. The detection of *Eucarya* in the microcosms was in agreement with the hybridization analysis of Fry et al. (1997) who reported *Eucarya* made up 6 to 14% of the microbial community in anaerobic groundwater from deep aquifers. While the nature and function of *Eucarya* observed in the microcosms is unknown, the detection of a consistent fraction suggests that these organisms were not directly affected by the treatments applied. Possibly, these *Eucarya* could be anaerobic protozoa grazing on the microbial populations that were stimulated in the microcosms.

Comparing the phylogenetic probe and chemical analyses shows that both toluene and NO_3^- stimulated microbial activity, but only the former had a significant effect on community structure at the phylum/subclass level. The lack of community structure shifts associated with NO_3^- supplementation may have reflected the widespread distribution of denitrification abilities, and/or phylogenetic overlap with organisms mediating other anaerobic processes. Further studies are needed to establish whether or not differing impacts of NO_3^- supplementation on community structure may be anticipated based on intrinsic characteristics of the environment and/or microbial community.

The consistent effect of toluene on altering microbial community structure in both the contaminated and pristine sediments indicated that organisms able to grow anaerobically on this compound were not uniformly distributed across the phylogenetic groups examined. Furthermore, the fact that community structure alterations induced by exposure to toluene were the same with or without nitrate addition suggested that the phylotypes stimulated in either sediment type were able to couple toluene degradation to energy conserving processes in addition to respiratory denitrification. Collectively, these results may reflect diversity in toluene degradation pathways within the phylotypes stimulated and/or the potential for these pathways to be coupled with multiple TEAPs. While the microbial community structures in the pristine and contaminated microcosms were similar in being significantly affected by toluene exposure, the patterns of these shifts were clearly distinct. Presumably, these differences were at least partly attributable to the impacts of prior exposure to hydrocarbon contamination and/or anaerobic conditions. It was also clear, however, that community structures in the toluene-amended pristine and contaminated microcosms did not resemble those of field samples from the pristine and contaminated regions, the latter of which were rather similar to each other. Incongruities such as these might be expected given that the microcosms were designed to accentuate community responses to individual environmental variables (e.g., toluene exposure) whereas the field samples represented the summation of a more complex series of environmental interactions acting over vastly different temporal and spatial scales.

VI. Conclusions
Results from our two-year study demonstrate that spatial variations in electron-accepting processes exist in both pristine and BTEX-contaminated portions of a shallow wetland aquifer at Fort McCoy, WI. The steep vertical gradients in both BTEX and redox zones in the plume indicate limited vertical mixing and distinct spatial zonation of biodegradation reactions. In this study, comparison of the redox patterns in pristine and contaminated portions of the aquifer

demonstrates that, although BTEX exerts the highest demand for electron acceptors, oxidation of natural organic matter in the wetland also contributes to utilization of DO and nitrate. Consideration of spatial variations in redox processes is important for calculations of assimilative capacity. Assimilative capacity calculations will also be more accurate if non-BTEX losses due to oxidation of natural organic matter, as well as oxidation of non-BTEX organic compounds in the plume, is considered. Even if electron acceptors are utilized to degrade only BTEX, and not other organic compounds in the plume, the total BTEX that can potentially be degraded in the shallow zone is around 8 mg/l, which is significantly less than the highest BTEX concentrations at the site (20 mg/l). If the natural processes are considered in calculations, the amount of BTEX that can be degraded decreases to around 7 mg/l. Thus, results of this study suggest that even though intrinsic bioremediation is not sufficient for complete remediation of the existing plume, it contributes to decreased BTEX concentrations in some areas of the plume.

To evaluate if biodegradation could be enhanced via addition of electron acceptors, we conducted three tracer experiments using bromide as a conservative tracer and nitrate and sulfate as potential electron acceptors. Results of the tracer experiments indicate that after a lag period, toluene, m, p-xylenes, and ethylbenzene degraded under nitrate-reducing conditions, but o-xylene and benzene remained recalcitrant. In the sulfate tracer experiment, loss of toluene, m, p-xylenes, and o-xylene was measured, but loss of sulfate was not, suggesting that either the amount of sulfate (~5 mg/l) needed to biodegrade BTEX was low and loss was masked by background sulfate concentrations (5-10 mg/l) or that the BTEX loss occurred under another electron-accepting process (Fe(III)-reduction or methanogenesis. Microcosm experiments are being designed to investigate this issue and are also being used to evaluate if benzene will degrade at all anaerobically at this field site.

Simulation of BTEX and electron acceptors at the site was accomplished using MODFLOW (McDonald and Harbaugh, 1988) to simulate flow and RT3D (Clement, 1997) to simulate transport and biodegradation. Results of the calibration show that field and simulated distribution of BTEX and redox zones match relatively well, with a few exceptions: 1) loss of sulfate and methanogenesis was slightly underpredicted and 2) the highest field Fe(II) values occur 20 m downgradient from the source area, while the highest simulated Fe(II) concentrations occur at the source. This may be due to a depleted reservoir of mineral-bound Fe(III) in the source zone. This model will be used as the base case for future simulations in support of design of an enhanced bioremediation system.

Hybridization analysis of aquifer samples with phylogenetic probes allowed identification of the dominant phylotypes comprising the microbial community. Phylogenetic probes were also used to in microcosm experiments detect significant shifts in community structure resulting from a single, relatively short-term exposure to toluene. These studies demonstrated that alterations in aquifer microbial communities resulting from specific anthropogenic perturbances can be inferred from microcosm studies combining chemical and phylogenetic probe analysis, and in the case of hydrocarbon contamination, may facilitate identification of organisms important for in situ biodegradation processes. Further work integrating microcosm and field experiments is needed to determine how differences in length of exposure to contaminants, contaminant concentration and/or chemical heterogeneity, and the spatial-temporal hydrogeologic heterogeneities that are inherent to aquifers may affect community structure patterns observed in these systems.

Comparison of first-order rate constants for toluene and nitrate loss using data collected from the tracer tests and microcosm experiments (**Table 13**) indicate that average first-order rate

constants derived from the tracer experiments are slightly lower than those derived from the microcosm experiments and that lag times are generally longer in the field.

Application of a variety of experimental tools has helped us to better understand the effects of microbial populations on the spatial distribution of electron acceptor and BTEX concentrations in a petroleum-contaminated wetland aquifer, and the effects of BTEX and electron acceptors on the microbial community structure. Results of these experiments will be used in further modeling studies to test the effects of different treatment scenarios, such as addition of nitrate into the plume, on BTEX concentrations.

References cited

Amann, R., W. Ludwig, and K.-H. Schleifer. 1994. Identification of uncultured bacteria: A challenging task for molecular taxonomists. ASM News 60: 360-365.

Anderson, R.T., J.N. Rooney-Varga, C.V. Gaw, and D.R. Lovley. 1998. Anaerobic benzene oxidation in the Fe(III) reduction zone of petroleum-contaminated aquifers. *Environ. Sci. Technol. 32*(9): 1222-1229.

Barbaro, J.R., J.F Barker, L.A. Lemon, and C.I. Mayfield. 1992. Biotransformation of BTEX under anaerobic, denitrifying conditions: Field and laboratory observations. *Jour. Contam. Hydrol. 11*: 245-272.

Barker, J.F., G.C. Patrick, and D. Major. 1987. Natural attenuation of aromatic hydrocarbons in a shallow sand aquifer. *Ground Water Monit. Rev. 7*: 64-71.

Batterman, G. 1986. Decontamination of polluted aquifers by biodegradation. In J.W. Assink and W.J. van den Brink, eds., 1985 International TNO Conference on Contaminated Soil, Nijhoff, Dordrecht, the Netherlands: 711-722.

Beller, H.R., M. Reinhard and D. Grbic-Galic. 1992 Metabolic by-products of anaerobic toluene degradation by sulfate-reducing enrichment cultures. *Appl. Environ. Microbiol. 58*(9): 3192-3195.

Birge, W.R. 1998. Estimating evapotranspiration rates using the water-table hydrograph method, Fort McCoy, Wisconsin. Unpublished independent study report, University of Wisconsin-Madison.

Borden R.C., C.A. Gomez, and M.T. Becker. 1995. Geochemical indicators of bioremediation. *Ground Water 33*(2): 180-189.

Brownell KA. 1997. Written communication.

Carey, G.R., P.J. Van Geel, and J.R. Murphy. 1998. BioRedox: A Coupled Biodegradation-Redox Model for Simulating Natural and Enhanced Bioremediation of Organic Pollutants. Conestoga-Rovers & Associates.

Chapelle F.H., P.B. McMahon, N.M. Dubrovsky, R.F. Fujii, E.T. Oaksford, and D.A. Vroblesky. 1995. Deducing the distribution of terminal electron-accepting processes in hydrologically diverse groundwater systems. *Water Resour. Res. 31*(2): 359-371.

Clement, T.P. 1997. RT3D (Version 1.0): A Modular Computer Code for Simulating Reactive Multispecies Transport in 3-Dimensional Groundwater Systems. Pacific Northwest National Laboratory, PNNL-SA-11720.

Coates, J. D., E. J. P. Phillips, D. J. Lonergan, H. Jenter, and D. Lovely. 1996. Isolation of *Geobacter* species from diverse sedimentary environments. *Appl. Environ. Microbiol. 62*:

3557-3559.

DeWild J. 1997. Underground storage tank investigation of a central fuel storage facility (Building 219), six petroleum, oil and lubrication stations and their associated pipeline, Fort McCoy, Wisconsin. Prepared in cooperation with the Fort McCoy Environmental and Natural Resources Division.

Fry, N. K., J. K. Fredrickson, S. Fishbain, M. Wagner, and D. A. Stahl. 1997. Population structure of microbial communities associated with two deep, anaerobic, alkaline aquifers. *Appl. Environ. Microbiol. 63*: 1498-1504.

Gottshalk, G. 1986. Bacterial Metabolism. Springer-Verlag, New York.

Hanson, R. S., and J. A. Phillips. 1981. Chemical Composition, p. 328-364. *In* P. Gerhardt et al. (eds.), Manual of Methods for General Bacteriology. American Society for Microbiology, Washington, D.C.

Hutchins, S.R. 1991. Biodegradation of monoaromatic hydrocarbons by aquifer microorganisms using oxygen, nitrate, or nitrous oxide as the terminal electron acceptor. *Appl. Environ. Microbiol. 57*(8): 2403-2407.

Hutchins S.R., W.C. Downs, J.T. Wilson, G.B. Smith, D.A. Kovacs, D.D. Fine, R.H. Douglass, and D.J. Hendrix. 1991. Effect of nitrate addition on biorestoration of a fuel-contaminated aquifer: Field demonstration. *Ground Water 29*(4): 571-590.

Lovley, D.R., J.C. Woodward, and F.H. Chapelle. 1994. Stimulated anoxic biodegradation of aromatic hydrocarbons using Fe(III) ligands. *Nature 370*: 128-131.

Lovley, D.R., J.C. Woodward, and F.H. Chapelle.1996. Rapid anaerobic benzene oxidation with a variety of chelated Fe(III) forms. *Appl. Environ. Microbiol. 62*(1): 288-291.

Lovley, D. R., and D. J. Lonergan. 1990. Anaerobic oxidation of toluene, phenol, and *p*-cresol by the dissimilatory iron-reducing organism GS-15. *Appl. Environ. Microbiol. 61*:1858-1964.

Lovley, D. R., S. J. Giovannoni, D. C. White, J. E. Chamoine, E. J. Phillips, Y. A. Goby, and S. Goodwin. 1993. *Geobacter metallireducens*, a microorganism capable of coupling the complete oxidation of organic compounds to the reduction of iron and other metals. *Arch. Microbiol.* 159: 336-344.

Major, D.W., C.I. Mayfield, and J.F. Barker. 1988. Biotransformation of benzene by denitrification in aquifer sand. *Ground Water 26*(1): 8-14.

McDonald, M.G. and A.W. Harbaugh. 1988. A Modular Three Dimensional Finite-Difference Ground-Water Flow Model: U.S. Geological Survey Techniques of Water Resources Investigations, book 6, chap. A1, 579p.

Naik, R. R, F. M. Murillo, J. F. Stolz. 1993. Evidence for a novel nitrate reductase in the dissimilatory iron-reducing bacterium *Geobacter metallireducens*. FEMS Microbiol. Lett. 106:53-58.

National Research Council. *In situ* bioremediation, when does it work? National Academy Press, Washington, D.C. 1994.

Newell, C.T., R.K. MacLeod, and J.R. Gonzales. 1996. BIOSCREEN: Natural Attenuation Decision Support System. U.S. Environmental Protection Agency, EPA/600/R-96/087. National Risk Management Research Laboratory, Office of Research and Development, U.S. Environmental Protection Agency, Cincinnati, OH.

Rifai, H.S., C.J. Newell, J.R. Gonzales, S. Dendrou, B. Dendrou, L. Kennedy, and J.T. Wilson. 1998. BIOPLUME III: Natural Attenuation Decision Support System. EPA/600/R-98/010. National Risk Management Research Laboratory, Office of Research and Development, U.S. Environmental Protection Agency, Cincinnati, OH.

Reinhard M., S. Shang, P.K. Kitanidis, E. Orwin, G.D. Hopkins, and C.A. Lebron. 1997. In situ biotransformation under enhanced nitrate- and sulfate-reducing conditions. *Environ. Sci. Technol. 31*: 28-36.

RUST, Inc. 1994. Wellhead Protection Area Study, Fort McCoy, Monroe County, Wisconsin. Prepared for the U.S. Army Engineer District and the Fort McCoy Military Reservation.

Schreiber, M.E., J.M. Bahr, M. Zwolinski, Y. Shi, W.J. Hickey, and K.A. Brownell. 1997. Field and laboratory studies of BTEX bioremediation under denitrifying conditions. *Proceedings of the Fourth International Symposium on In Situ and On-Site Bioremediation 5*: 13-19.

Schreiber, M.E. unpublished data.

Shi, Y, Zwolinksi, M., Schreiber, M.E., Bahr, J.M., Sewell, G.W., and W.J. Hickey. In press. Molecular analysis of microbial community structure in pristine and contaminated aquifers: Field and laboratory microcosm studies. *Appl. Environ. Microbiol.*

Stites W. and L.W. Chambers. 1991. A method for installing miniature multilevel sampling wells. *Ground Water 29*:430-432.

Tsai, Y. -L., and B. H. Olsen. 1991. Rapid method for direct extraction of DNA from soil and sediments. *Appl. Environ. Microbiol. 57*:1070-1074.

Weatherburn, M. W. 1967. Phenol-hypochlorite reaction for the determination of ammonia. *Anal. Chem. 39*: 971-974.

Wiedemeier, T.H., J.T. Wilson, D.H. Kampbell, R.N. Miller, and J.E. Hansen. 1995. Technical Protocol for Implementing Intrinsic Remediation with Long-Term Monitoring for Natural Attenuation of Fuel Contamination Dissolved in Groundwater. Revision 0. Air Force Center for

Environmental Excellence, San Antonio, TX.

Wilson, B.H, J.T. Wilson, D.H. Kampbell, B.E. Bledsoe, and J.M. Armstrong. 1990. Biotransformation of monoaromatic and chlorinated hydrocarbons at an aviation gasoline spill site. *Geomicrobiol. J. 8*: 225-240.

Zheng, C. 1990. MT3D: A Modular Three-Dimensional Transport Model for Simulation of Advection, Dispersion, and Chemical Reactions of Contaminant in Groundwater Systems. Report to the U.S. Environmental Protection Agency, Ada OK.

Zheng, D., E. W. Alm, D.A. Stahl, and L. Raskin. 1996. Characterization of universal small-subunit rRNA hybridization probes for quantitative molecular microbial ecology studies. *Appl. Environ. Microbiol. 62*: 4504-4513.

Figure captions

Figure 1. Location map of Fort McCoy WI and site map of POL (Petroleum, Oils and Lubricants) Station 6 with total BTEX concentrations (mg/l) in April 1998.

Figure 2. Concentrations of electron acceptors (DO, NO_3, Fe(II), and SO_4) in four multilevel samplers along the uncontaminated transect A - A' (see Figure 1 for transect location) in April, 1998. Dashed lines separate shallow, intermediate, and deep groundwater zones.

Figure 3. Concentrations (mg/l) of BTEX, benzene, and toluene at four multilevels along the contaminated transect B - B' (see Figure 1 for transect location) in April, 1998. Dashed lines separate shallow, intermediate, and deep groundwater zones.

Figure 4. Concentrations of electron acceptors (DO, NO_3, Fe(II), and SO_4) in four multilevel samplers along the contaminated transect B - B' (see Figure 1 for transect location) in April, 1998. Dashed lines separate shallow, intermediate, and deep groundwater zones. Shallow groundwater has highest concentrations of BTEX (> 1 mg/l); intermediate and deep zones contain BTEX concentrations less than 0.1 mg/l.

Figure 5. Comparison of contaminated vertical BTEX and redox patterns in monitoring well MW8 with multilevel sampler MLA4. Data collected in September 1997.

Figure 6. Schematic of injection set-up a) 96NB test, b) 97NB test, and c) 97SB test.

Figure 7. Horizontal and vertical hydraulic gradients for the field site and the tracer site (inset).

Figure 8. 96NB test: breakthrough curves, a) shallow zone (2.3 m bgs), b) intermediate zone (2.6), and deep zone (2.9 m).

Figure 9. 97NB test: breakthrough curves in intermediate zone (2.6 m bgs).

Figure 10. 97SB test: breakthrough curves in shallow zone (2.3 m bgs). Sulfate was analyzed using the turbidimetric method (0.5, 1.1 m) or by ion chromatography (7.1, 8.4 m).

Figure 11. 96NB test: nitrate utilization in shallow (2.3 m bgs), intermediate (2.6 m), and deep (2.9 m) zones

Figure 12. 97NB test: a) nitrate and b) TEX losses in intermediate zone (2.6 m bgs).

Figure 13. 97SB test: Toluene and xylene losses in shallow zone (2.3 m bgs).

Figure 14. Calibrated heads, run plume19d. Contours are in meters.

Figure 15. BTEX concentrations (mg/l), averaged 1995 to 1998.

Figure 16. Electron acceptor concentrations, averaged 1995-1998, for DO, nitrate, dissolved

Fe(II), and sulfate. Contours are approximate. All concentrations are in mg/l.

Figure 17. Five-year simulated BTEX and electron acceptor distributions (plume 19d). All concentrations are in mg/l.

Figure 18. Molecular analysis of DNA extracted from field samples of pristine and contaminated aquifer material. A. DNA yields in crude extracts from field samples of the indicated aquifer materials. Data plotted are means of extracts made on duplicate samples ± standard deviation. B. Relative abundance (universal probe-normalized signals) of domains and subgroups (phylum and subclass levels) in the pristine and contaminated samples. The sums of domain and subgroup hybridization signals (± standard deviation) given in the box above the figure. Legend for probe target groups: UNI: universal; EUC: *Eucarya*; ARC: *Archaea*; BAC: Bacteria; ALF: α-*Proteobacteria*; B+G: β+γ-*Proteobacteria*; SRB: sulfate-reducing bacteria; HGC: high G+C gram-positive bacteria. Data are means of duplicate determinations ± standard deviation.

Figure 19. Molecular analysis of DNA extracted from microcosms established with pristine aquifer material. A. Total yields of DNA in crude extracts from microcosm with the indicated amendment; data plotted are means of extracts made on duplicate microcosms ± standard deviation. B. Relative abundance of domain or subgroups (phylum and subclass levels) as determined by hybridization to the indicated probe.

Figure 20. Molecular analysis of DNA extracted from microcosms established with contaminated aquifer material. A. Total yields of DNA in crude extracts from microcosm with the indicated amendment; data plotted are means of extracts made on duplicate microcosms ± standard deviation. B. Relative abundance of domain or subgroups (phylum and subclass levels) as determined by hybridization to the indicated probe.